Dynamics of exciton-spin injection, transfer, and relaxation in self-assembled quantum dots of CdSe coupled with a diluted magnetic semiconductor layer of $Zn_{0.80}Mn_{0.20}Se$

A. Murayama,* T. Furuta, K. Hyomi, I. Souma, and Y. Oka
Institute of Multidisciplinary Research for Advanced Materials, Tohoku University, Sendai 980-8577, Japan

D. Dagnelund, I. A. Buyanova, and W. M. Chen
Department of Physics, Chemistry and Biology, Linköping University, 58183 Linköping, Sweden
(Received 11 January 2007; revised manuscript received 17 April 2007; published 4 May 2007)

We study the dynamics of exciton-spin injection, transfer, and relaxation in self-assembled quantum dots (QDs) of CdSe coupled with a diluted magnetic semiconductor (DMS) layer of $Zn_{0.80}Mn_{0.20}Se$, where spin-polarized excitons can be injected from the DMS into the QDs. The degree of circular polarization P of excitonic photoluminescence (PL) at 5 T in the coupled QDs exhibits a rapid increase with increasing delay time, up to +0.3 at 25 ps after the pulse excitation of the DMS by a linearly polarized light. This development of a positive P value directly reflects the spin-injection dynamics from the DMS, since the intrinsic polarization of the QD excitons due to Zeeman splitting is $P \sim -0.1$ when only the QDs are selectively excited. The P value gradually decays with time after reaching its maximum, as a result of the exciton-spin relaxation with a time constant of 800 ps in the QDs. Time-resolved circularly polarized PL spectra immediately after the pulse excitation directly show the exciton-energy dependence of the spin-injection dynamics in the QD ensemble, where two-dimensional-like QDs with higher exciton energies show higher receptivity to the spin-polarized excitons than three-dimensional-like dots with lower exciton energies. A rate equation analysis reveals all time constants responsible for the spin-injection dynamics. We deduce a time constant of 10 ps for the spin injection. The spin-injection efficiency of 0.94 is also obtained, which corresponds to the ratio between the number of the spin-polarized excitons responsible for the rise of the positive P value in the QD emission and the total number of the excitons injected from the DMS. Moreover, we observe that interdot exciton transfer significantly affects the P value within the QD emission band after the fast spin injection, in addition to the spin relaxation within the QDs.

DOI: 10.1103/PhysRevB.75.195308 PACS number(s): 78.47.+p, 78.55.Et, 78.67.Hc

I. INTRODUCTION

Great attention has been paid to self-assembled quantum dots (QDs) of compound semiconductors, owing to their new intriguing physical properties, as well as their potential applications for efficient optical devices that exploit the strong quantum confinement effects. Moreover, spin states of carriers and excitons have extensively been studied in the QDs during the previous decade, as they are regarded as being among the most important material candidates for realizing spin-electronic devices and quantum computing.[1,2] Both fundamental interest and technological relevance of the QDs have motivated intense research efforts worldwide on the dynamics of spin-polarized carriers and excitons in these systems. Spin-relaxation times of electrons and excitons have been shown to be as long as 1 ns or longer in the QDs, which is significantly longer than typical spin-relaxation times of several tens of picoseconds in quantum wells.[3–6] Interesting spin dynamics has also been reported for the exciton or the electron in CdSe QDs.[7,8] Therefore, there is an important advantage in exploring QDs for future applications based on spin manipulation. In addition to this, correlations of the electronic spin states among dots are also found to be very attractive.[9–13] Spin dynamics in these coupled-QD systems with a diluted magnetic semiconductor (DMS) can be largely affected by the correlation of the wave functions of the spin-polarized carriers or excitons. As a result, interesting phenomena such as an antiferromagnetic coupling of exciton spins have been reported.[10,14] The electronic states of each self-assembled dot correlate through tunneling and energy-transfer processes even in a single-layer structure, if the sheet density of the dot is high, leading to close dot separations.[15,16] The high-density QD system holds great potential for device applications, because of their high intensities of optical signals, such as photoluminescence (PL), electroluminescence, and lasing. Dense QDs of CdSe, for example, can be grown on a ZnSe-buffer layer in a manner of self-assembled growth, resulting in a typical sheet density of 10^{10}–10^{11} cm^{-2}.[16,17]

As mentioned above, long spin-relaxation times of carriers or excitons are very advantageous for transient spin storage in future spintronic semiconductor devices based on spin manipulation. However, for manipulation of spins, one also needs to create and rapidly flip the spins. For this, a DMS can be employed, where photoexcited carriers and excitons are highly spin polarized and the spin direction can be easily controlled by an external magnetic field applied to the DMS. The spin injection, which is the transport of spin-polarized carriers or excitons into a nonmagnetic semiconductor, has been experimentally demonstrated in layered structures using the DMS.[18,19] The spin injection is also very attractive from the viewpoint of fundamental semiconductor physics. Recently, we have studied the spin-injection dynamics in double quantum wells (QWs) of the DMS by means of time-resolved circularly polarized PL and pump-probe absorption spectroscopy under magnetic fields.[20–24] We show that the

spin-injection efficiency is strongly affected by the spin dynamics such as spin polarization in the DMS QW, spin tunneling or transfer, and spin relaxation in the nonmagnetic QW. On the other hand, application and rapid reversal of local magnetic fields for the DMS are possible by, e.g., using hybrid nanostructures of ferromagnetic materials with controlled magnetic shape anisotropies.[25–29] Therefore, we can manipulate the spin states of the carriers or excitons in the QDs using a QD structure coupled with a DMS, if we efficiently and rapidly inject the spin-polarized carriers or excitons from the DMS into the QDs. The exciton-spin injection has been demonstrated from DMS to nonmagnetic semiconductor quantum disks with a lateral diameter of 30 nm coupled through a tunneling barrier, which was fabricated from a double quantum well by electron-beam lithography.[30,31] Efficient exciton-spin injection has also recently been reported from a DMS layer to self-assembled CdSe QDs.[32] Recently, we have realized efficient electron-spin injection by exploiting a type-II band alignment between a DMS QW and CdSe QDs and LO-phonon-assisted resonant tunneling.[33–35] However, unfortunately, our understanding of spin dynamics in the coupled-QD system with DMS is still rather limited, in particular, the dynamics of spin injection and relaxation in a laterally dense QD system where electronic spin states correlate among the dots.

In this work, we have prepared dense self-assembled CdSe QDs coupled with a ZnMnSe-based DMS layer and studied the spin dynamics such as spin injection, spin transfer, and spin relaxation by means of circularly polarized transient PL under magnetic fields. Here, we use a DMS-$Zn_{0.80}Mn_{0.20}Se$ layer as a source of spin-polarized excitons with the exciton energy almost equal to the band-gap energy of a ZnSe spacer inserted between the DMS and the QDs. Such design of the band alignment enables us to directly measure the spin dynamics in the coupled-QD ensemble with the DMS layer using ultrafast spin-resolved optical spectroscopy, where the exciton spin can efficiently be injected from the DMS immediately after the pulse excitation. In this way, we are able to demonstrate fast and efficient injection of the spin-polarized excitons from the DMS into the QDs. In addition, we can evaluate the exciton-energy dependence of the spin-injection efficiency within the QD emission band originating from the QDs of various shapes and sizes. The subsequent exciton-spin relaxation can also be studied after the fast spin injection via the interdot exciton transfer and the intradot spin-relaxation processes.

II. EXPERIMENTAL PROCEDURES

The sample structure studied in this work, denoted below as the spin-injection structure, was grown by molecular-beam epitaxy on a GaAs (100) substrate and is schematically shown in Fig. 1. The $Zn_{0.80}Mn_{0.20}Se$ layer with a thickness of 100 nm was grown on a ZnSe-buffer layer, followed by a spacer layer of ZnSe with a thickness of 10 nm. Then, the CdSe layer with a thickness of three monolayers was grown using an atomic layer epitaxy technique on the ZnSe spacer. Here, the self-assembled QDs were successfully formed by stacking of the CdSe layer on the ZnSe surface resulting

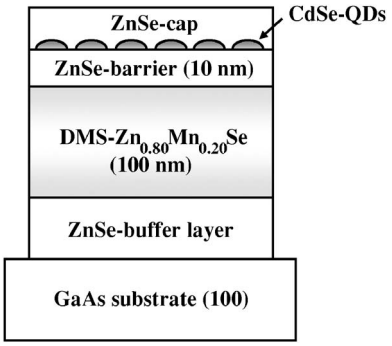

FIG. 1. A schematic illustration of the spin-injection structure containing the CdSe QDs coupled with the DMS-$Zn_{0.80}Mn_{0.20}Se$ layer.

from the Stranski-Krastanow (SK)-growth mode. The dot formation was directly confirmed by continuous observations of reflection high-energy electron difraction images from streak to spotty patterns. The average diameter of the QDs is estimated to be about 3 nm judging from the energy of their PL emission, if we assume a spherical shape of the dots.[36] Finally, a cap layer of ZnSe was deposited on top of the QD layer. A CdSe-QD layer without the DMS layer, denoted below as the reference sample, was also grown and was fabricated into mesa-shaped nanopillars with lateral dimensions less than 100 nm by electron-beam lithography so that it is suitable for micro-PL (μ-PL) measurements.

Figure 2 shows a schematic illustration of the excitonic energy diagram of the spin-injection structure. At low temperatures and high magnetic fields, excitons generated in the DMS layer are spin polarized resulting from the giant Zeeman effects. The exciton PL shows σ^+-circular polarization from the lower-energy spin state (with the magnetic quantum number $m_j=-1/2, +3/2$, defined for the exciton state) of the DMS. These spin-polarized excitons can be injected into the QDs driven by the potential difference of 0.3 eV between the

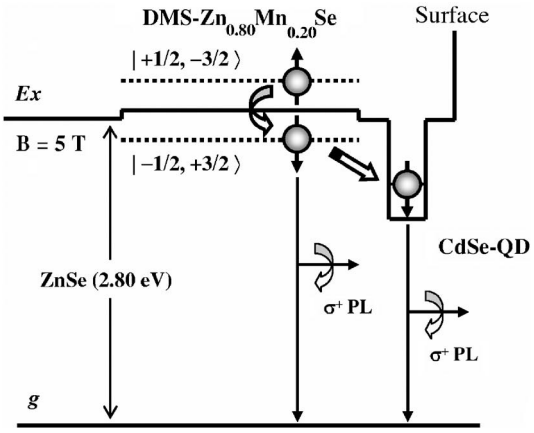

FIG. 2. The excitonic energy diagram at magnetic fields of 0 T (solid line) and 5 T (dotted line) in the coupled-QD system, where "Ex" and "g" denote the exciton states and the crystal ground state, respectively. A possible injection process of spin-polarized excitons and the resultant circularly polarized PL are also shown by open and solid arrows, respectively. The magnetic quantum numbers are defined for the spin-split exciton states of the DMS.

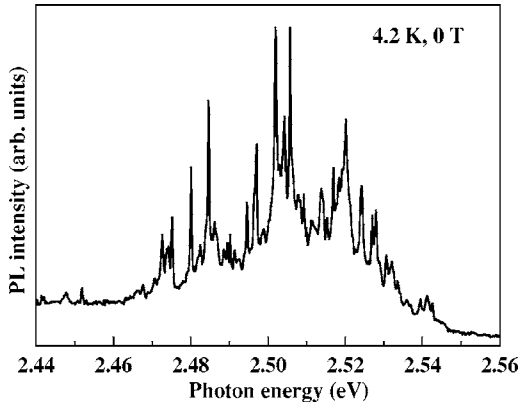

FIG. 3. Excitonic PL spectrum of the mesa-shaped reference sample of a single CdSe-QD layer without the DMS, measured at 4.2 K and 0 T by the micro-PL technique.

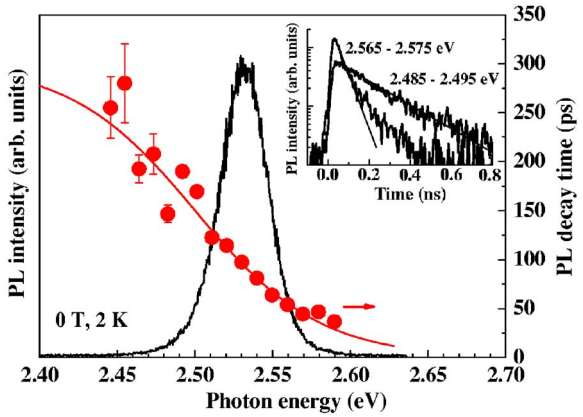

FIG. 4. (Color online) Excitonic PL spectrum (solid line) and the PL decay times (closed circles) as a function of photon energy at 2 K and 0 T from the spin-injection structure. The energy of the excitation photons from linearly polarized light pulses was 2.75 eV, which is below the exciton band-gap energies of both the DMS and the ZnSe spacer. The solid line for the closed circles shows the fitting calculated by Eq. (1) in the text. The inset shows typical PL decay curves at higher and lower detection energies, from which the PL decay times were obtained (solid lines).

DMS and QDs. The resulting exciton-spin injection can be monitored by the σ^+-polarized PL (and PL polarization) from the QDs, because the intrinsic circular polarization of the exciton PL in the CdSe QDs favors σ^- that is opposite to that of the injected excitons from the DMS.

The spin dynamics of the structures was studied by employing time-resolved circularly polarized PL spectroscopy at 2 K under magnetic fields up to 5 T in the Faraday geometry. The excitation was performed using second-harmonic light pulses of a mode-locked Ti:sapphire laser with a pulse width of 150 fs and repetition rate of 82 MHz. The wavelength of the excitation light was tuned in the range of 390–450 nm. The time-resolved PL spectrum was captured by a streak camera and the time resolution of the system was 15 ps. A μ-PL system using a cw-InGaN laser with a wavelength of 408 nm was also used at 4.2 K for the reference sample under magnetic fields up to 5 T in the Faraday geometry. The energy resolution of the μ-PL spectrum was 0.4 meV. The spot size of the excitation light was 1 μm.

III. RESULTS AND DISCUSSION

A. Spin dynamics in CdSe QDs

To selectively study the spin dynamics of the QDs, we used the photoexcitation at 2.75 eV that is below the band-gap energies of the DMS and the ZnSe spacer. Before this selective-excitation study, a μ-PL spectrum from the reference sample of a single CdSe-QD layer is shown in Fig. 3. The spectral width of the narrowest PL lines is 0.4 meV, which is limited by the spectral resolution of our μ-PL measurement. It is interesting to note that the spectral intensity in the higher-energy region of the emission band is lower than that in the middle- and lower-energy regions in the CdSe-QD ensemble. This feature agrees with our transient PL results, as will be described below. From the μ-PL measurements, we can estimate the sheet density of the dots to be in the range of 10^{11} cm^{-2}. We have estimated the sheet densities of our CdSe-QD samples from the number of PL peaks observed by μ-PL in the mesa-shaped samples with diameters (50–100 nm) known from a scanning electron microscope. The circularly polarized PL spectra under magnetic fields indicate a g value of excitons for the individual CdSe QDs, where the σ^--polarized emission peak lies at the lower-energy side, that is, the exciton ground state in each dot. The exciton g value is deduced to be 1.7 for these CdSe QDs from the magnetic-field dependence of the energy separation between the σ^-- and σ^+-polarized μ-PL peaks. This g value is similar to that of 1.6 previously reported in the literature.[37]

First, we shall present our results on spin dynamics of the CdSe-QD ensemble in the spin-injection structure. A broad PL band with a width of 40 meV was observed in macro-PL experiments, see Fig. 4. It originates from the overlapping narrow exciton PL lines from the individual QDs, as it is typically seen in the μ-PL spectrum of the reference sample shown in Fig. 3. The observed decay time τ of the QD excitonic PL at 0 T is also shown in Fig. 4, which is found to critically depend on the exciton energy of the QDs. A systematic increase of τ from 40 to 280 ps can be observed with a decrease in the exciton energy within this QD emission band. This variation of τ can be attributed to interdot exciton transfer from the dots with higher exciton energies to the ones with lower energies, occurring when the sheet density of the CdSe dots is rather high such as in our case. The distribution of the exciton energy is due to the size and shape distributions of the QDs. Here, in our CdSe-ZnSe system, two types of the dot shape have been reported.[38–40] One is a two-dimensional (2D)-like dot mainly due to lateral fluctuations of the Cd content. The other one is an island-shaped dot formed by the SK-growth mode. This SK-type island induces strong exciton localization resulting from the higher Cd concentration and the larger volume. The exciton tunneling has been pointed out as the exciton-transfer mechanism since barrier heights among the dots are relatively low, resulting from compositional fluctuations and shallow localization potentials.[40] In addition to this, the energy transfer of excitons is also possible. When the interdot separation becomes

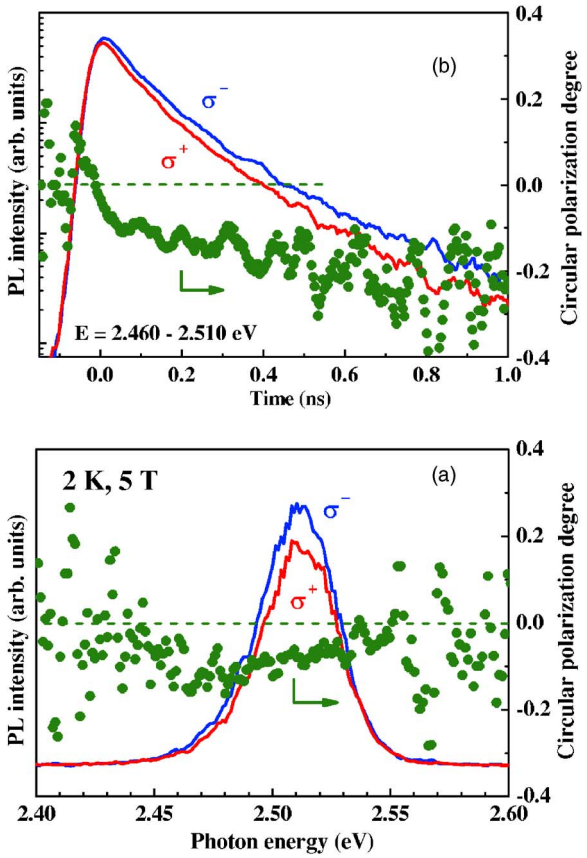

FIG. 5. (Color online) (a) Time-integrated circularly polarized exciton PL spectra (σ^+ and σ^-) and the degree of circular polarization (P, closed circles) at 2 K and 5 T with the same excitation condition as in Fig. 4. (b) The transient PL intensities and P are also shown for the detection energy of 2.460–2.510 eV.

small at a high dot density, energy-transfer processes of excitons between various dots can take place and should be taken into consideration. Thermally activated escape and recapture of excitons, on the other hand, can be negligible under our experiment conditions at a low temperature of 2 K. The observed decay times of the excitons from the QDs are analyzed by a model calculation originally accounting for the energy transfer in a dense QD system,[41] as follows:

$$\tau(E) = \frac{\tau_r}{1 + \exp[(E - E_{mc})/E_0]}. \quad (1)$$

Here, E_{mc} is the energy at which the radiative lifetime equals the exciton-transfer time, E_0 is a constant expressing the average localization energy in the QD system, and τ_r denotes the radiative lifetime of the QDs. The best fit of the experimental results is shown by the solid line in Fig. 4, yielding the following fitting parameters; τ_r=300 ps, E_{mc}=2.50 eV, and E_0=40 meV. The complex potential fluctuations seem to approximately lead to an exponential distribution of the exciton localization energy.

At a magnetic field of 5 T, PL from the QD excitons becomes σ^- polarized, as shown in Fig. 5(a). Here, the excitation was also performed selectively for the QDs under the same condition as that in Fig. 4. Similar to the decay time τ, the circular polarization degree P is also dependent on the exciton energy. P is defined by

$$P = \frac{I(\sigma^+) - I(\sigma^-)}{I(\sigma^+) + I(\sigma^-)}, \quad (2)$$

where I denotes the circularly polarized PL intensity. The P value decreases from 0 at the higher-energy edge of the QD-PL emission band to −0.1 in the lower-energy region. This σ^--polarization property originates from the Zeeman splitting of the exciton states in the CdSe QDs, leaving the σ^--active spin state lowest in energy, and thus favorably populated. This variation of the P value with exciton energy seems to correlate with and to a large extent can be accounted for by the variation of the decay time with exciton energy. The P value is determined by the population difference between the higher-lying σ^+-active spin state and the lower-lying σ^--active spin state of the QD excitons. This population is, in turn, governed by the competition between the spin relaxation between the two spin states and the exciton decay. If the latter dominates over the former, the communication between the two spin states driven by the spin relaxation is negligible and their population is determined by their difference in generation. In the present case, when a linearly polarized light was employed, an equal number of the excitons was created for both spin states, leading to a vanishing degree of the PL polarization. This scenario seems to be able to explain the experimental observation of $P \sim 0$ at the highest-energy edge of the QD-PL band, correlated with the shortest decay time of about 40 ps. To justify the assumption that the spin-relaxation time is much longer than 40 ps, we have directly monitored the spin-flip process between the two spin states by studying the transient behavior of the PL polarization for the QD excitons at the lowest energy. It can be seen from Fig. 5(b) that the P value is close to zero immediately after the pulsed photoexcitation using a linearly polarized light. It gradually develops a negative value, with time caused by the spin relaxation, from which the exciton-spin-relaxation time of 800 ps can be estimated. We have measured time-resolved and circularly polarized exciton PL under magnetic fields in a single layer of CdSe QDs.[16,33,34] The PL decay curves can be fitted by a rate equation calculation based on the population decays of spin-polarized excitons in a two-level system taking into account a time constant of the spin relaxation. The obtained spin-relaxation time of 800 ps is much longer than the interdot transfer time of 40 ps for the QDs giving rise to the excitonic PL at the highest energy, explaining the vanishing PL polarization within the spectral range [see Fig. 5(a)]. With decreasing exciton energy, the decay time is shown to increase, see Fig. 4. This can lead to an increasing population difference between the spin states due to the increasing importance of the spin relaxation, and thus a more negative P value, assuming that the spin-relaxation time is not significantly altered with the exciton energy.

B. Spin-injection dynamics from DMS into CdSe QDs

Now, we shall present our results on the spin-injection dynamics in the spin-injection structure using macroscopic

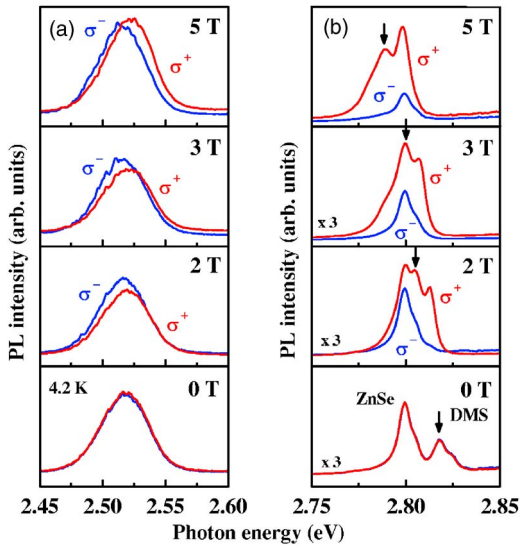

FIG. 6. (Color online) (a) Circularly polarized cw PL of the excitons from the coupled QDs and (b) the DMS layer where the spectral peaks are indicated by arrows, obtained at 4.2 K and various magnetic fields. The excitation photon energy was 3.05 eV, which is above both the DMS and ZnSe band-gap energies. The PL emission from the ZnSe layers appears at 2.80 eV and is independent of the magnetic-field strength.

time-resolved PL measurements. In these experiments, the excitation was performed using linearly polarized light pulses with energy above the band-gap energies of both $Zn_{0.80}Mn_{0.20}Se$ and ZnSe. The resulting circularly polarized PL spectra, obtained at 4.2 K and various magnetic fields, are shown in Fig. 6 for the QDs (a) and the DMS layer (b). The DMS layer shows a typical giant Zeeman shift of the exciton peaks, where the PL energy decreases by 30 meV at 4.2 K with increasing magnetic field up to 5 T. At 3 T, the PL energy from the lower-energy spin state $(-1/2, +3/2)$ becomes lower than the exciton energy of the ZnSe layers. In accordance with this, the excitonic PL from the QDs shows an increase in the circular polarization degree P. The P value becomes positive in the higher-energy region of the emission band, which is opposite the intrinsic polarization of the QDs observed in the case of selective excitation of the QDs, as shown in Fig. 5. Therefore, the appearance of this σ^+-polarized PL provides experimental evidence for exciton-spin injection from the DMS layer to the QDs.

The results of the time-resolved PL measurement at 5 T are shown in Figs. 7–9. Figure 7 shows circularly polarized exciton PL intensities and P vs time by detecting higher- and lower-energy regions of the coupled-QD emission band, where the linearly polarized photoexcitation was performed at 3.17 eV [(c) and (d), above the DMS exciton energy] in comparison with the excitation at 2.75 eV [(a) and (b), below the DMS exciton energy]. The PL intensity decays almost exponentially at the higher exciton energy, when the QDs are selectively excited (a). Compared with this, when we excite the DMS, as well as the ZnSe barrier, a nonexponential decay of PL with much higher intensity can be observed, in addition to the appearance of the σ^+ polarization (c). This nonexponential decay suggests complicated exciton dynamics involving exciton injection from the DMS and ZnSe with various time constants. The transient change in the P value, from positive to negative, and its dependence on the exciton energy are very interesting. They directly reflect the exciton-spin dynamics including the spin injection, transfer, and relaxation. The detailed dynamics of the spin injection and subsequent spin transfer and relaxation in the QD ensemble can be clearly seen from time-resolved circularly polarized PL spectra, as shown in Fig. 8. At the early stage after the pulse excitation, from 0 to 85 ps, the PL intensity with σ^+ polarization is markedly higher than that with σ^- polarization. Positive values of P up to +0.3 are observed particularly in the high-energy region of the QD emission band. After this time domain, the PL intensity with σ^- polarization gradually becomes higher than that with σ^+ polarization, leading to negative P values, especially in the low-energy region. The positive P values observed immediately after the laser pulses directly indicate the exciton-spin injection, where the injection occurs mainly within such a short time period. The fast spin-injection process is facilitated by the

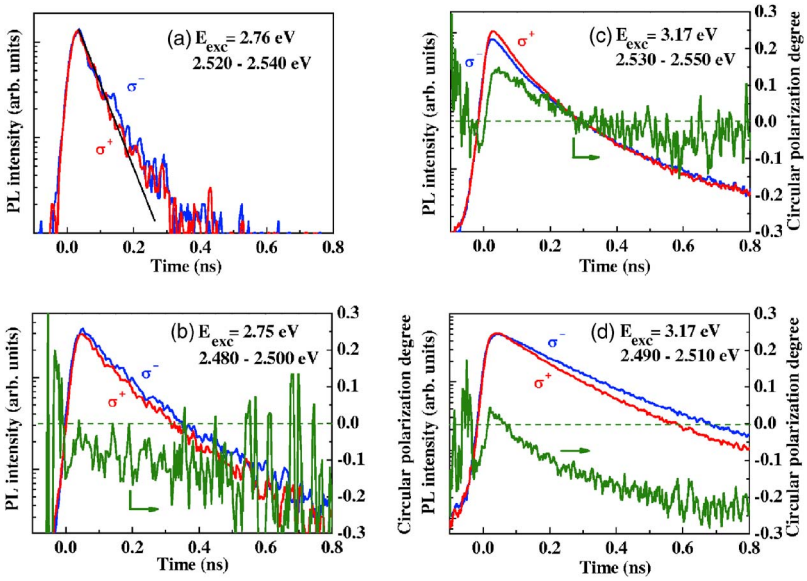

FIG. 7. (Color online) Decay curves of the circularly polarized exciton PL intensities and P at 2 K and 5 T, by detecting the higher- and lower-energy regions of the coupled-QD emission band. The photoexcitation using linearly polarized light pulses was performed [(a) and (b)] at 2.75 eV, which is below both the DMS and ZnSe exciton energies, [(c) and (d)] and at 3.17 eV, which is above both the DMS and ZnSe band-gap energies. The solid line in (a) is a guide for the eyes indicating a singly exponential decay.

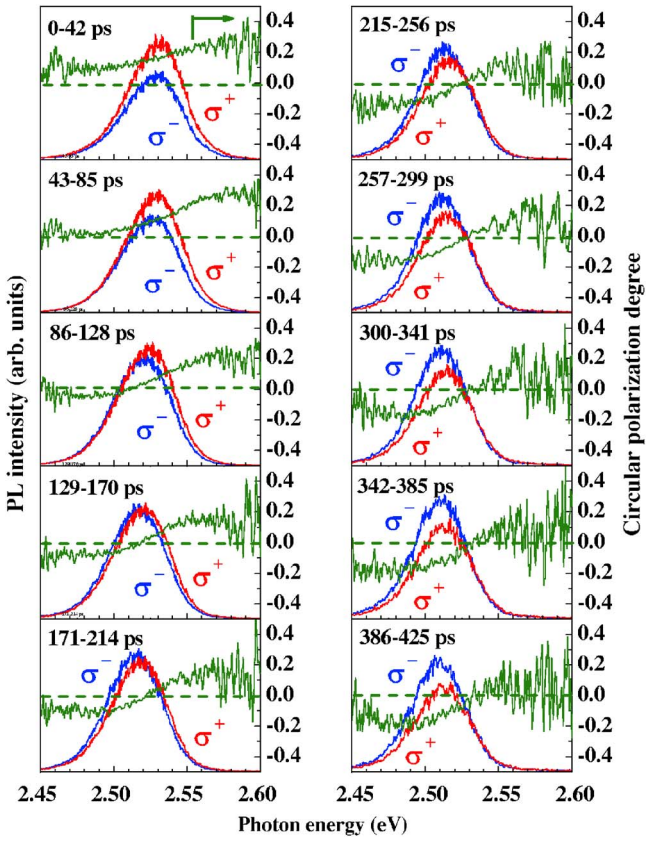

FIG. 8. (Color online) Time-resolved circularly polarized exciton PL spectra and the P values vs photon energy at 2 K and 5 T in the coupled QDs, where the excitation was performed at 3.17 eV by using linearly polarized pulses. The time window for the accumulation of the PL spectra is indicated in each panel.

large penetration of the wave function of the spin-polarized excitons in the DMS into the QDs, when the energy of the lower-energy spin state of the DMS is slightly lower (10 meV for the exciton energy) than the energy level of the ZnSe spacer. On the other hand, the development of the

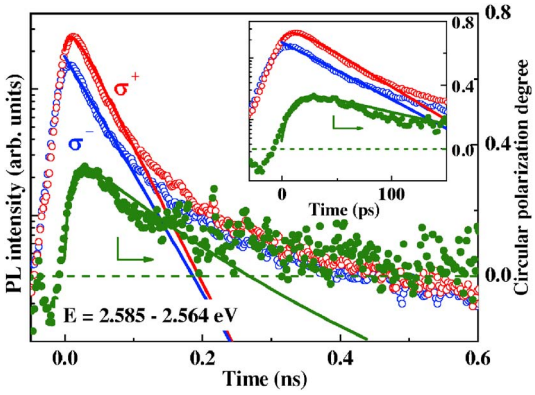

FIG. 9. (Color online) Circularly polarized exciton PL intensities (open circles) and P (closed circles) as a function of time for the spectral window of 2.564–2.585 eV, measured at 5 T in the coupled QDs. The solid lines are the calculations using the rate equations for the PL intensities and P. The inset shows a close-up over the shorter time period.

negative P value after a longer delay time is caused by the spin relaxation inside the dots.

From these time-resolved circularly polarized PL spectra, it is possible to obtain information on the probability of spin injection from the DMS to various QDs. As can be seen within the time window of 0–42 ps shown on the top left of Fig. 8, the P value tends to decrease gradually as the detection energy decreases, from 0.3 to 0.1, where the effect of the spin relaxation can be negligible since the time constant of the spin relaxation is much longer than this time scale of the detection. Therefore, this tendency shows the importance of the dot shape in the spin-injection probability. The dot shape embedded in the wetting layer at the higher-energy region in the QD emission band is mainly 2D-like while is 3D-like at the lower-energy region, resulting from the SK-growth mode. Several effects can contribute to the observed dependence. For example, it can be related to different spin depolarizations at the interfaces with the 2D and 3D dots. In the 3D dots, the lattice is relaxed to some extent at the bottom interface, resulting from the SK-growth mode. Therefore, the atom-scale interface quality can be degraded, while it is not significantly affected in the strained 2D dot embedded in the wetting layer. The existence of defects at the interface can reduce the spin-injection efficiency, as shown earlier between ZnMnSe and AlGaAs.[42] Moreover, a cross-sectional area of the dot is generally larger for the 2D-like dot at the interface between the dot and the ZnSe spacer layer than the 3D-like one. Therefore, a larger number of the spin-polarized excitons can be injected from the DMS layer into the 2D-like dots. The number of nonpolarized excitons that is directly excited in the dots is approximately proportional to the dot volume. If the dot volume is not significantly different, this situation results in a higher P value in the 2D-like dot. Also, the shape of the 3D dots is islandlike and opens into the cap layer, where a larger number of nonpolarized excitons can be migrated from the cap layer, as compared to the 2D dots. Moreover, the continuity of the exciton wave function in the DMS layer is higher for the 2D dots than for the 3D-like ones. This means that the spin-polarized exciton wave function in the DMS can penetrate into the 2D-like dots more easily than into the 3D dots. From the above arguments, we can expect a tendency of higher receptivity to the spin injection for the 2D-like dots with the higher exciton energy than for the 3D-like dots. After this fast spin injection, the P value decreases gradually in the middle- and low-energy regions of the emission band. In these energy regions, the exciton-transfer time is longer than that in the high-energy region. Therefore, the spin relaxation affects the P value observed, as discussed above in Sec. III A. It should be noted that we did not observe a noticeable difference in the spin dynamics between the smaller 2D dots and larger SK dots except for the spin injection, and the spin-relaxation time is similar in these dots. Therefore, effects of the dot shape on the spin-relaxation time are likely not significant in this case because it is the freezing of the carrier motion that largely affects the spin relaxation in the dot and the dot shape may not be important as long as the three-dimensional confinement acts sufficiently on carriers. In the spin-injection dynamics, as can be seen in time-resolved spectra of the circular polarization degree P in Fig. 8, we have observed a clear exciton-

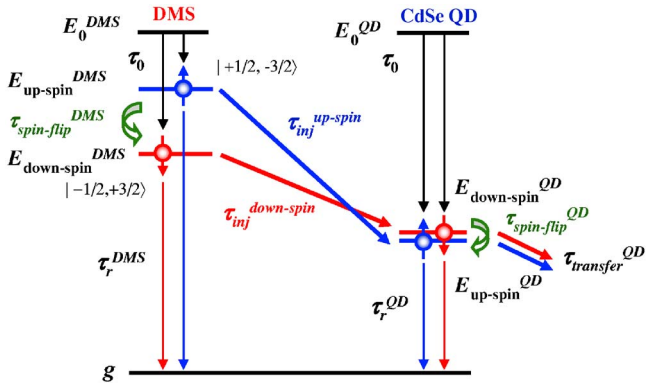

FIG. 10. (Color online) A rate equation model for the exciton-spin injection and relaxation in the spin-injection structure, where the interdot exciton transfer is taken into account (see text).

energy dependence of P, which coincides with the exciton-energy dependence of the exciton lifetime as shown in Fig. 4.

Figure 9 shows the circularly polarized PL intensities and P as a function of time after the linearly polarized pulse excitation, where the spectral window is set as 2.564–2.585 eV, corresponding to the higher-energy edge of the QD emission band. As can be seen, the σ^+-polarized PL intensity increases just after the excitation due to the spin injection from the DMS, while σ^--polarized PL intensity decreases monotonically. The P value rapidly increases beyond 0.3 with increasing time after the pulse excitation. After reaching its maximum at 25 ps, the P value decays gradually, which can be attributed to the spin relaxation in the QDs.

C. Rate equation analysis of spin injection dynamics

In order to obtain a quantitative understanding of the exciton-spin injection dynamics, a detailed analysis of the transient PL intensity and polarization is performed based on the model shown in Fig. 10, with the following coupled rate equations:

$$\frac{dN_0^{DMS}}{dt} = -\frac{2}{\tau_0}N_0^{DMS}, \tag{3}$$

$$\frac{dN_0^{QD}}{dt} = -\frac{2}{\tau_0}N_0^{QD}, \tag{4}$$

$$\frac{dN_{up\text{-}spin}^{DMS}}{dt} = \frac{1}{\tau_0}N_0^{DMS} - \frac{1}{\tau_{spin\text{-}flip}^{DMS}}N_{up\text{-}spin}^{DMS} - \frac{1}{\tau_{inj}^{up\text{-}spin}}N_{up\text{-}spin}^{DMS} - \frac{1}{\tau_r^{DMS}}N_{up\text{-}spin}^{DMS}, \tag{5}$$

$$\frac{dN_{down\text{-}spin}^{DMS}}{dt} = \frac{1}{\tau_0}N_0^{DMS} + \frac{1}{\tau_{spin\text{-}flip}^{DMS}}N_{up\text{-}spin}^{DMS} - \frac{1}{\tau_{inj}^{down\text{-}spin}}N_{down\text{-}spin}^{DMS} - \frac{1}{\tau_r^{DMS}}N_{down\text{-}spin}^{DMS}, \tag{6}$$

$$\frac{dN_{down\text{-}spin}^{QD}}{dt} = \frac{1}{\tau_0}N_{QD} + \frac{1}{\tau_{inj}^{down\text{-}spin}}N_{down\text{-}spin}^{DMS} - \frac{1}{\tau_{transfer}^{QD}}N_{down\text{-}spin}^{QD} - \frac{1}{\tau_{spin\text{-}flip}^{QD}}N_{down\text{-}spin}^{QD} - \frac{1}{\tau_r^{QD}}N_{down\text{-}spin}^{QD}, \tag{7}$$

$$\frac{dN_{up\text{-}spin}^{QD}}{dt} = \frac{1}{\tau_0}N_{QD} + \frac{1}{\tau_{inj}^{up\text{-}spin}}N_{up\text{-}spin}^{DMS} - \frac{1}{\tau_{transfer}^{QD}}N_{up\text{-}spin}^{QD} + \frac{1}{\tau_{spin\text{-}flip}^{QD}}N_{down\text{-}spin}^{QD} - \frac{1}{\tau_r^{QD}}N_{up\text{-}spin}^{QD}. \tag{8}$$

Here, the time constants of the spin injection are included as $\tau_{inj}^{up\text{-}spin}$ and $\tau_{inj}^{down\text{-}spin}$ for the up (higher-energy) and down (lower-energy) spin states of the DMS. $\tau_{transfer}^{QD}$ denotes the time constants of the interdot exciton transfer. $\tau_{spin\text{-}flip}^{QD}$ and $\tau_{spin\text{-}flip}^{DMS}$ represent the exciton-spin relaxation (spin flip) in the QDs and DMS, respectively. The following experimentally determined values are used in the analysis:

(a) Recombination lifetimes of $\tau_r^{DMS}=60$ ps and $\tau_r^{QD}=300$ ps for the DMS and QD excitons, respectively, which are determined from the decay dynamics of the DMS and QD excitons in the absence of the spin injection and interdot exciton transfer.

(b) The interdot transfer time $\tau_{transfer}^{QD}=50$ ps, which is deduced from the exciton PL decay time in the highest-energy region.

(c) The exciton-spin-relaxation time of $\tau_{spin\text{-}flip}^{QD}=800$ ps for the QD, as deduced in Sec. III A.

(d) The spin-flip time in the DMS $\tau_{spin\text{-}flip}^{DMS}=1$ ps, which was obtained by our pump-probe absorption measurement on a single quantum well of DMS.[43] [This rapid exciton-spin relaxation is caused by ultrafast spin relaxation of a heavy hole (hh) mainly due to LO-phonon scattering among the spin-split states of the hh. This is also supported by the fact that no PL can be observed from the higher-energy spin state in the DMS layer, since a dark exciton is immediately formed after the ultrafast relaxation of the hh.]

(e) An initial relaxation time $\tau_0=0.1$ ps from hot exciton states to the monitored exciton ground state is assumed, which is sufficiently shorter than the time resolution of our PL measurement.

The calculations using the rate equations can be fitted to the experimental time dependences of both PL intensity and the P value, as shown in Fig. 9. As can be seen, the fitted curves agree well with the experimental results within the time period up to 150 ps. From the best fit, the following fitting parameters can be determined: the spin-injection times of $\tau_{inj}^{up\text{-}spin}=8$ ps for the up-spin exciton and $\tau_{inj}^{down\text{-}spin}=10$ ps for the down-spin exciton, the initial population ratio of the hot excitons between the DMS layer and QDs N_0^{QD}: $N_0^{DMS}=7:5$. The value of N_0^{QD} includes the nonpolarized excitons injected from the nonmagnetic ZnSe cap and barrier layers, as well as those directly excited in the QDs. N_0^{DMS} denotes the total number of the excitons involved in this spin-injected process in the DMS layer. Though the time constant $\tau_{inj}^{up\text{-}spin}=8$ ps is comparable to $\tau_{inj}^{down\text{-}spin}=10$ ps, the injection of the up-spin excitons is strongly suppressed because of the ul-

trafast spin relaxation within the DMS layer ($\tau_{spin\text{-}flip}^{DMS}=1$ ps). Most excitons therefore relax immediately from the up-spin state to the down-spin one inside the DMS before the spin injection, leading to high spin injection efficiency. We can estimate the spin-injection efficiency $\eta_{inj}^{down\text{-}spin}$ that is defined as the ratio between the number of the down-spin excitons and the total number of the excitons injected from the DMS into the dots detected in the higher-energy emission region:

$$\eta_{inj}^{down\text{-}spin}=\frac{N_{inj}^{down\text{-}spin}}{N_{inj}^{up\text{-}spin}+N_{inj}^{down\text{-}spin}}, \tag{9}$$

$$N_{inj}^{up\text{-}spin}=\frac{N_0}{2}\left[\frac{1}{1+(\tau_{inj}^{up\text{-}spin}/\tau_{spin\text{-}flip}^{DMS})}\right], \tag{10}$$

$$N_{inj}^{down\text{-}spin}=\left\{\frac{N_0}{2}+\frac{N_0}{2}\left[\frac{1}{(\tau_{spin\text{-}flip}^{DMS}/\tau_{inj}^{up\text{-}spin})+1}\right]\right\}\times\left[\frac{1}{1+(\tau_{inj}^{down\text{-}spin}/\tau_{r}^{DMS})}\right]. \tag{11}$$

By using the time constants determined from the rate equation analysis described above, we obtain $\eta_{inj}^{down\text{-}spin}=0.94$.

Here, we consider the exciton tunneling from the DMS into the QDs since the experimental PL decay curves can be interpreted by the rate equation calculation based on the above exciton-transfer model. Separate tunneling of carriers and the exciton tunneling have both been experimentally elucidated with their relative importance depending on the QW structure, as revealed in previous studies for the transfer dynamics of spin-polarized excitons in DMS-based double QWs.[20–24] In the present coupled-QD structure with the DMS layer, the ZnSe barrier height is low (12 meV at 5 T) from the DMS side. This situation allows the exciton transfer rather than the individual carrier transfer since such a barrier height is sufficiently lower than the exciton binding energy in the DMS layer (~20 meV).

As can be seen in Fig. 9, the calculated results show discrepancies from the experimental time dependences after 150 ps, when the PL intensities and the P value become higher than the calculated ones. These results indicate additional exciton-spin injection channels with relatively slow time constants. To shed light on the possible origin of the additional channels, the decay curve of the σ^+-polarized PL from the down-spin exciton state of the DMS layer at 5 T is shown in Fig. 11. The decay curve is clearly nonexponential and the emission remains beyond 800 ps after the excitation. The magnetization of Mn spins is close to saturation at this 5 T, as shown in the inset of Fig. 11. Therefore, effects of the magnetic polaron formation can be neglected in the interpretation of the spin-injection dynamics. We should point out that potential fluctuations due to inhomogeneous alloying should be significant in the DMS layer of $Zn_{0.80}Mn_{0.20}Se$ due to the rather high Mn content. The microscopic potential fluctuations create localization sites for carriers and excitons with various potential depths, leading to the formation of localized excitons and localized electron-hole (e-h) pairs with varying decay times. Therefore, two possible origins can be considered for the slower spin-injection processes.

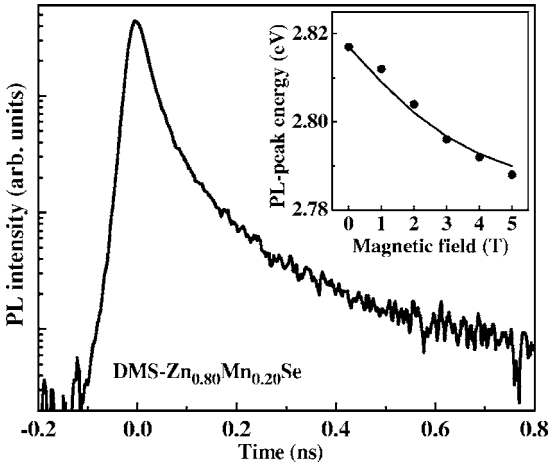

FIG. 11. Decay of the σ^+-circularly polarized PL from the excitons in the DMS layer coupled with the QDs, obtained at 2 K and 5 T. An inset shows the magnetic-field dependence of the PL peak energy. A solid line is a calculation using a Brillouin function.

One is the slower migration of the spin-polarized and localized excitons from relatively inner parts of the DMS layer (with a total thickness of 100 nm), which is farther away from the QDs. The rather broad PL spectral width of 20 meV of the DMS excitons evidences the presence of the potential fluctuations. The other origin is spin-conserving energy transfer from the localized excitons and localized e-h pairs in the DMS layer, which was experimentally shown by using type-II double quantum wells with DMS.[22] This spin-conserving energy transfer also gives slower spin injection because of the long lifetime of the localized excitons and localized e-h pairs in the DMS layer, as is seen in Fig. 11.

D. Effects of interdot exciton transfer on the spin-injection dynamics

Figure 12 shows circularly polarized PL spectra and the P-value variation in the PL emission band of the coupled

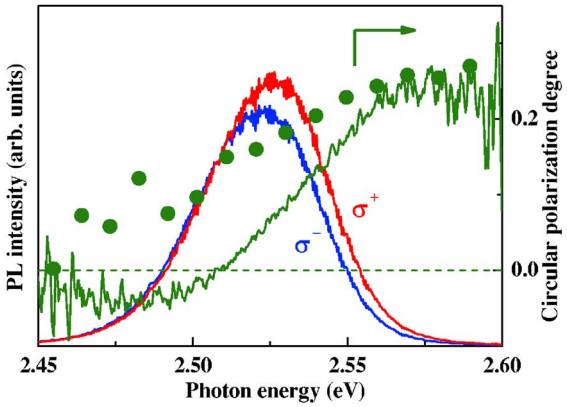

FIG. 12. (Color online) Circularly polarized exciton PL spectra integrated over the time window of 0–200 ps and the P values vs photon energy (solid lines) for the coupled QDs, obtained at 2 K and 5 T. The solid circles show the calculated P values based on the same simplified spin-injection model illustrated in Fig. 10.

QDs, integrated over the time range of 0–200 ps. In the high-energy region above 2.55 eV, the P values calculated by the rate equations agree well with the experimental values. This is consistent with the fact that the rate equation analysis can reproduce the experimental decay curves for the high-energy region of the QD emission band, as shown in Fig. 9. At lower energies, we observe a systematic decrease in the P value from +0.25 to −0.04 with decreasing exciton energy. This observation can at least partly be explained by the interdot exciton transfer occurring in the studied structure due to the high dot density, as discussed in Sec. III A. The time constant of the exciton transfer is much faster (~40 ps) than the spin-relaxation time of 800 ps in the dots on the high-energy side. Therefore, the time-integrated P values in the high-energy region remain high since the spin-polarized excitons injected from the DMS transfer to other dots before losing their spins. However, the P values in the middle- and low-energy regions decrease markedly due to the spin relaxation in each dot since the exciton-transfer time becomes longer and comparable to the spin-relaxation time as the exciton energy decreases. The calculated P values (the solid circles in Fig. 12) based on the same rate equations used in Sec. III C show fair agreement with the experimental tendency of this exciton-energy dependence of the P value, where the exciton-energy dependence of the spin-relaxation and exciton-transfer times are included.

However, the discrepancies between the experimental P values and the calculated ones are apparent in the middle- and low-energy regions (see Fig. 12). It should be noted that the simplified model of the rate equation analysis employed here only includes the exciton transfer from the dot under consideration to other dots but not the other way around. Therefore, it is only appropriate for the QDs with the highest exciton energy. The observed discrepancies of the P value thus indicate the existence of multiple paths of the exciton transfer in this dense dot system, which should be considered when analyzing the results in the middle- and lower-energy regions of the QD emission band. In reality, the spin-polarized excitons with various degrees of spin depolarization can be transferred from the dots with higher exciton energies to those with lower exciton energies. As a result, the P value observed can appear more negative than that deduced from the calculation based on the simplified model, explaining at least partly the discrepancies in Fig. 12. Moreover, the efficiency of the spin injection from the DMS to the QDs at the lower energies can be markedly different from that to the QDs at the higher energies, as indicated in Fig. 7. A thorough understanding of the discrepancies therefore requires substantial further efforts both experimentally and theoretically. The possibility of spin flip during the interdot exciton transfer is interesting and, in principle, cannot be completely ruled out. However, we were not able to obtain experimental evidence either proving or disproving the involvement of spin flip during the interdot exciton transfer. Further studies are required for a better understanding of detailed spin dynamics during the interdot spin transfer in the QD ensemble.

IV. SUMMARY

We have studied exciton-spin dynamics in self-assembled QDs of CdSe coupled with a DMS-$Zn_{0.80}Mn_{0.20}Se$ layer. The excitonic PL of the QDs at 5 T shows an increase in the degree of circular polarization P up to +0.3 at 25 ps after the pulse excitation of the DMS by using linearly polarized light. This provides direct evidence for the spin injection from the DMS to the QDs, as the intrinsic P of the QDs when the QDs are selectively excited is ~−0.1 resulting from the negative g value of −1.7. The time-resolved circularly polarized PL studies clearly show the exciton-energy dependence of the spin-injection dynamics in the QD ensemble, where 2D-like QDs with higher exciton energies possess higher probability of spin injection than 3D-like dots. With the aid of the rate equation analysis, we deduce the time constants responsible for the spin injection in the coupled-QD system. A fast time constant of 10 ps is determined for the spin injection. The spin-injection efficiency of 0.94 is also obtained for the QDs with the highest exciton energy. We observe that the interplay between the interdot exciton transfer and the spin relaxation with the QD plays a crucial role in the P value observed in the spin-injection dynamics. $P \sim +0.2$ is obtained for the higher-energy region of the QD emission band with the exciton-transfer time of 40 ps, and it decreases down to −0.04 with decreasing exciton energy. The spin dynamics elucidated in this study contains rich physical aspects about relations between the spin injection, spin transfer, and spin relaxation in a correlated QD system coupled with a DMS layer.

ACKNOWLEDGMENTS

This work is supported in part by the Ministry of Education, Science, and Culture, Japan. Financial support by the Swedish Research Council (VR) and the Swedish Foundation for International Cooperation in Research and Higher Education (STINT) is greatly appreciated.

*Author to whom correspondence should be addressed. Electronic address: murayama@tagen.tohoku.ac.jp

[1] D. Loss and D. P. DiVincenzo, Phys. Rev. A **57**, 120 (1998).
[2] A. Imamoglu, D. D. Awschalom, G. Burkard, D. P. DiVincenzo, D. Loss, M. Sherwin, and A. Small, Phys. Rev. Lett. **83**, 4204 (1999).
[3] M. Paillard, X. Marie, P. Renucci, T. Amand, A. Jbeli, and J. M. Gérard, Phys. Rev. Lett. **86**, 1634 (2001).
[4] S. Mackowski, T. A. Nguyen, H. E. Jackson, L. M. Smith, J. Kossut, and G. Karczewski, Appl. Phys. Lett. **83**, 5524 (2003).
[5] M. Kroutvar, Y. Ducommun, D. Heiss, M. Bichler, D. Schuh, G. Abstreiter, and J. J. Finley, Nature (London) **432**, 81 (2004).
[6] J. M. Elzerman, R. Hanson, L. H. Willems van Beveren, B. Witkamp, L. M. K. Vandersypen, and L. P. Kouwenhoven, Nature (London) **430**, 431 (2004).
[7] T. Flissikowski, A. Hundt, M. Lowisch, M. Rabe, and F. Hen-

neberger, Phys. Rev. Lett. **86**, 3172 (2001).
[8] I. A. Akimov, D. H. Feng, and F. Henneberger, Phys. Rev. Lett. **97**, 056602 (2006).
[9] A. Tackeuchi, Y. Nakata, R. Sasou, K. Mase, T. Kuroda, and N. Yokoyama, Physica E (Amsterdam) **10**, 32 (2001).
[10] A. Tackeuchi, T. Kuroda, R. Sasou, Y. Nakata, and N. Yokoyama, Physica B **314**, 25 (2002).
[11] M. Obert, B. Wild, G. Bacher, A. Forchel, R. André, and L. S. Dang, Appl. Phys. Lett. **80**, 1322 (2002).
[12] G. Ortner, M. Bayer, A. Larionov, V. B. Timofeev, A. Forchel, Y. B. Lyanda-Geller, T. L. Reinecke, P. Hawrylak, S. Fafard, and Z. Wasilewski, Phys. Rev. Lett. **90**, 086404 (2003).
[13] H. Xiong, Z. H. Chen, K. Hyomi, I. Souma, Y. N. Zhang, L. X. Sun, Q. J. Ren, L. H. Bai, S. H. Huang, F. Z. Wang, A. Murayama, Y. Oka, and S. C. Shen, J. Lumin. **119-120**, 193 (2006).
[14] S. Lee, H. S. Lee, J. Y. Lee, M. Dobrowolska, and J. K. Furdyna, Appl. Phys. Lett. **86**, 033114 (2005).
[15] A. Tackeuchi, Y. Nakata, S. Muto, Y. Sugiyama, T. Usuki, Y. Nishikawa, N. Yokoyama, and O. Wada, Jpn. J. Appl. Phys., Part 2 **34**, L1439 (1995).
[16] I. Souma, K. Kayanuma, K. Hyomi, K. Nishibayashi, A. Murayama, and Y. Oka, J. Supercond. **18**, 219 (2005).
[17] A. Hundt, J. Puls, and F. Henneberger, Phys. Rev. B **69**, 121309(R) (2004).
[18] R. Fiederling, M. Keim, G. Reuscher, W. Ossau, G. Schmidt, A. Waag, and L. W. Molenkamp, Nature (London) **402**, 787 (1999).
[19] Y. Ohno, D. K. Young, B. Beschoten, F. Matsukura, H. Ohno, and D. D. Awschalom, Nature (London) **402**, 790 (1999).
[20] K. Kayanuma, S. Shirotori, Z. H. Chen, T. Tomita, A. Murayama, and Y. Oka, Physica B **340-342**, 882 (2003).
[21] I. A. Buyanova, G. Y. Rudko, W. M. Chen, K. Kayanuma, A. Murayama, Y. Oka, A. A. Toropov, S. V. Sorokin, and S. V. Ivanov, Phys. Rev. B **71**, 165203 (2005).
[22] W. M. Chen, I. A. Buyanova, K. Kayanuma, K. Nishibayashi, K. Seo, A. Murayama, Y. Oka, A. A. Toropov, A. V. Lebedev, S. V. Sorokin, and S. V. Ivanov, Phys. Rev. B **72**, 073206 (2005).
[23] K. Nishibayashi, I. Souma, A. Murayama, and Y. Oka, Appl. Phys. Lett. **88**, 211108 (2006).
[24] T. Koyama, K. Kayanuma, I. Souma, A. Murayama, and Y. Oka, Appl. Phys. Lett. **88**, 212106 (2006).
[25] J. Kossut, I. Yamakawa, A. Nakamura, G. Cywiński, K. Fronc, M. Czeczott, J. Wróbel, F. Kyrychenko, T. Wojtowicz, and S. Takeyama, Appl. Phys. Lett. **79**, 1789 (2001).
[26] M. Sakuma, K. Hyomi, I. Souma, A. Murayama, and Y. Oka, J. Appl. Phys. **94**, 6423 (2003).
[27] M. Sakuma, K. Hyomi, I. Souma, A. Murayama, and Y. Oka, Appl. Phys. Lett. **85**, 6203 (2004).
[28] H. Schömig, A. Forchel, S. Halm, G. Bacher, J. Puls, and F. Henneberger, Appl. Phys. Lett. **84**, 2826 (2004).
[29] A. Murayama and M. Sakuma, Appl. Phys. Lett. **88**, 122504 (2006).
[30] A. Uetake, H. Ikada, T. Asahina, M. Sakuma, K. Hyomi, T. Tomita, A. Murayama, and Y. Oka, Phys. Status Solidi C **1**, 941 (2004).
[31] T. Tomita, A. Uetake, T. Asahina, K. Kayanuma, A. Murayama, and Y. Oka, J. Supercond. **18**, 405 (2005).
[32] J. Seufert, G. Bacher, H. Schömig, A. Forchel, L. Hansen, G. Schmidt, and L. W. Molenkamp, Phys. Rev. B **69**, 035311 (2004).
[33] A. Murayama, T. Asahina, K. Nishibayashi, I. Souma, and Y. Oka, Appl. Phys. Lett. **88**, 023114 (2006).
[34] A. Murayama, T. Asahina, K. Nishibayashi, I. Souma, and Y. Oka, J. Appl. Phys. **100**, 084327 (2006).
[35] T. Asahina, K. Kayanuma, K. Nishibayashi, I. Souma, K. Hyomi, A. Murayama, and Y. Oka, Phys. Status Solidi C **3**, 1114 (2006).
[36] Y. Kayanuma and H. Momiji, Phys. Rev. B **41**, 10261 (1990).
[37] V. D. Kulakovskii, G. Bacher, R. Weigand, T. Kümmell, A. Forchel, E. Borovitskaya, K. Leonardi, and D. Hommel, Phys. Rev. Lett. **82**, 1780 (1998).
[38] D. Schikora, S. Schwedhelm, D. J. As, K. Lischka, D. Litvinov, A. Rosenauer, D. Gerthsen, M. Strassburg, A. Hoffmann, and D. Bimberg, Appl. Phys. Lett. **76**, 418 (2000).
[39] M. Strassburg, Th. Deniozou, A. Hoffmann, R. Heitz, U. W. Pohl, D. Bimberg, D. Litvinov, A. Rosenauer, D. Gerthsen, S. Schwedhelm, K. Lischka, and D. Schikora, Appl. Phys. Lett. **76**, 685 (2000).
[40] M. Strassburg, M. Dworzak, H. Born, R. Heitz, A. Hoffmann, M. Bartels, K. Lischka, D. Schikora, and J. Christen, Appl. Phys. Lett. **80**, 473 (2002).
[41] C. Gourdon and P. Lavallard, Phys. Status Solidi B **153**, 641 (1989).
[42] R. M. Stroud, A. T. Hanbicki, Y. D. Park, G. Kioseoglou, A. G. Petukhov, B. T. Jonker, G. Itskos, and A. Petrou, Phys. Rev. Lett. **89**, 166602 (2002).
[43] A. Murayama, K. Seo, K. Nishibayashi, I. Souma, and Y. Oka, Appl. Phys. Lett. **88**, 261105 (2006).